



Received 21 May 2026

Accepted 12 June 2026

In memoriam Professor Manfred T. Reetz (1943–2026). This article is part of the collection Early Career Scientists in Structural Science.

Keywords: crystal structure; Hirshfeld atom refinement; non-spherical atomic form factors; 2,6-dimethylmorpholine; *meso* compound.

CCDC reference: 2561790

Supporting information: this article has supporting information at journals.iucr.org/e

Crystal structure of the *meso* compound (2*R*,6*S*)-4-(5-bromopyrimidin-2-yl)-2,6-dimethylmorpholine

Paul R. Palme,^a Richard Goddard,^b Markus Leutsch,^b Adrian Richter,^a Peter Imming^a and Rüdiger W. Seidel^{a*}

^aInstitut für Pharmazie, Martin-Luther-Universität Halle-Wittenberg, Wolfgang-Langenbeck-Str. 4, 06120 Halle (Saale), Germany, and ^bMax-Planck-Institut für Kohlenforschung, Kaiser-Wilhelm-Platz 1, 45470 Mülheim an der Ruhr, Germany. *Correspondence e-mail: ruediger.seidel@pharmazie.uni-halle.de

The title compound, C₁₀H₁₄N₃OBr, was prepared by a nucleophilic aromatic substitution reaction between 2,6-dimethylmorpholine and 2-chloropyrimidine, followed by bromination of the pyrimidine ring. The compound crystallizes in the monoclinic system (space group *P*2₁/*c*) with four molecules in the unit cell (*Z* = 4). The molecule exhibits approximate *C*_s point-group symmetry (r.m.s. deviation: 0.1072 Å). The arrangement of the molecules in the solid state is dominated by close packing. C–H···N contacts between pyrimidinyl rings in adjacent molecules with an *R*₂²(6) motif are encountered, whereas the bromine atom does not exhibit any short contacts that could be regarded as halogen bonds.

1. Chemical context

2,6-Dimethylmorpholine, usually the *cis* isomer, is a common building block in medicinal chemistry as it allows for modulating lipophilicity, basicity, metabolic stability and binding to the biological target. The antifungal agent amorolfin and the antineoplastic compound sonidegib are examples of approved and marketed drugs containing a *cis*-2,6-dimethylmorpholine group. In the context of our antimycobacterial drug discovery efforts, 4-arylmorpholine building blocks have attracted our interest (Palme *et al.*, 2025). We synthesized and crystallographically characterized (2*R*,6*S*)-4-(5-bromopyrimidin-2-yl)-2,6-dimethylmorpholine (**4**) in two steps from commercially available starting materials (Fig. 1), adapting an established route (Cheprakova *et al.*, 2014). The first step was a nucleophilic aromatic substitution (S_NAr) reaction between 2-chloropyrimidine (**1**) and 2,6-dimethylmorpholine hydrochloride (**2**) in the presence of a base to yield 2,6-dimethyl-4-(pyrimidin-2-yl)morpholine (**3**; Hanyu *et al.*, 2009). [The configuration of 2,6-dimethylmorpholine hydrochloride as purchased was unspecified, but ¹H and ¹³C NMR spectroscopy (see supporting information) indicate that only one isomer was present]. It is worth noting that Wei *et al.* (2019) reported the synthesis of **3** by a transition-metal-free cross-coupling

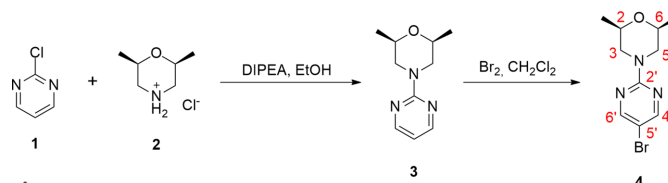
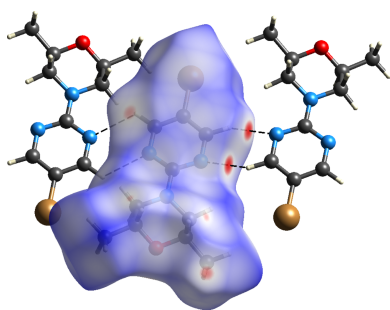
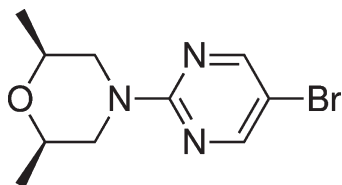


Figure 1
Two-step synthesis of **4**. DIPEA = *N,N*-Diisopropylethylamine (Hünig's base).

reaction of 2-cyanopyrimidine with 2,6-dimethylmorpholine, and that, recently, Hall *et al.* (2025) described a one-pot sequential desulfonylative fluorination of pyrimidine-2-sulfonyl fluoride followed by an S_NAr reaction with 2,6-dimethylmorpholine. Finally, bromination of **3** in the second step gave compound **4** in good yield. Synthesis of **4** from 5-bromo-2-chloropyrimidine and 2,6-dimethylmorpholine under S_NAr conditions has been described in the patent literature (Heng *et al.*, 2008; Yoshihara *et al.*, 2011; Wu *et al.*, 2015; You *et al.*, 2023; Shojaei *et al.*, 2023).



2. Structural commentary

Fig. 2 shows the molecular structure of **4** in the crystal. X-ray crystallography confirmed that the 2,6-dimethylmorpholine ring is *cis*-configured. As expected, it adopts a chair conformation with the two methyl groups in equatorial positions. The 2,6-dimethylmorpholine group and the pyrimidine ring are slightly inclined relative to one another about the C8–N4 bond, resulting in a r.m.s. deviation from exact molecular C_s point group symmetry of 0.1072 Å. The geometry at N4 of the morpholine ring deviates marginally from planarity, as indicated by $\Sigma(C-N-C) = 357.89$ (9)°, which is barely smaller than 360° expected for an ideal planar coordination. The pyramidal height, *i.e.* the perpendicular distance of N4 to the plane specified by C3, C5 and C8, is small [0.1198 (6) Å]. This indicates that the lone pair of N4 is conjugated with the aromatic system of the pyrimidine ring.

The high-frequency shift of the 1H NMR signal assigned to the equatorial H atoms at C3 and C5 (4.45–4.33 ppm) can most likely be attributed to an anisotropic shielding effect exerted by the lone pairs of N1 and N3. Such a high-frequency shift of the morpholine H-3_{eq}/H-5_{eq} signal was not observed for 2,6-dimethyl-4-phenylmorpholine (Yuan *et al.*, 2024) or other *cis*-

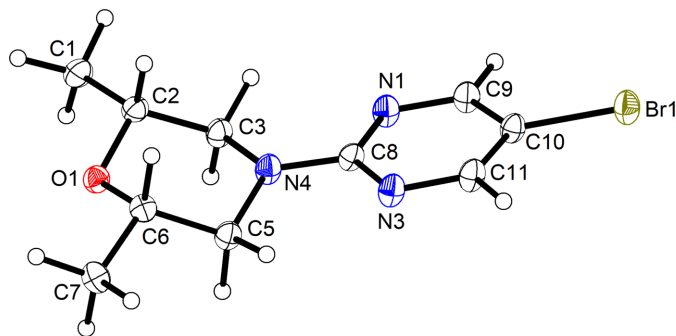


Figure 2
Molecular structure of **4** in the crystal. Displacement ellipsoids are drawn at the 50% probability level. H atoms are represented as small spheres of arbitrary radius.

Table 1
Hydrogen-bond geometry (Å, °).

$D-H\cdots A$	$D-H$	$H\cdots A$	$D\cdots A$	$D-H\cdots A$
C7–H7A \cdots O1 ⁱ	1.078 (12)	2.499 (12)	3.4295 (9)	143.9 (8)
C9–H9 \cdots N1 ⁱⁱ	1.065 (10)	2.580 (10)	3.2779 (9)	122.5 (7)
C11–H11 \cdots N3 ⁱⁱⁱ	1.095 (11)	2.423 (11)	3.3610 (9)	142.8 (8)

Symmetry codes: (i) $-x + 1, y + \frac{1}{2}, -z + \frac{1}{2}$; (ii) $-x + 2, -y + 1, -z + 1$; (iii) $-x + 1, -y + 2, -z + 1$.

2,6-dimethylmorpholine derivatives (Brügel, 1969). The C8–N4 bond is shorter than the corresponding C–N bond in 4-phenylmorpholine (WOXMOP; Jiang *et al.*, 2023) by 0.048 (2) Å.

3. Supramolecular features

The most prominent supramolecular feature in the crystal structure of **4** is weak C–H \cdots N hydrogen bonding between the pyrimidine rings of adjacent symmetry-related molecules (Fig. 3), resulting in centrosymmetric $R_2^2(6)$ motifs (Bernstein *et al.*, 1995). The geometric parameters listed in Table 1 suggest that the C11–H11 \cdots N3ⁱⁱⁱ hydrogen bond is more favourable than C9–H9 \cdots N1ⁱⁱ, as indicated by shorter H \cdots A and $D\cdots A$ distances and a $D-H\cdots A$ angle closer to linearity. In addition, a $C_{\text{methyl}}-H\cdots O_{\text{morpholine}}$ intermolecular short contact (C7–H7A \cdots O1ⁱ) can be identified. Such contacts are ubiquitous in crystal structures of organic molecules (Desiraju, 1995). Short contacts to bromine that could be interpreted as halogen bonds are not encountered.

A Hirshfeld surface analysis was undertaken to investigate close intermolecular contacts and supramolecular assembly in the crystal structure in a more objective and quantitative manner (Spackman & Jayatilaka, 2009). Fig. 4 shows the Hirshfeld surface mapped with the normalized contact distance (d_{norm}), whereby red, white and blue regions respectively indicate intermolecular contacts shorter, approximately equal and longer than the sum of the van der

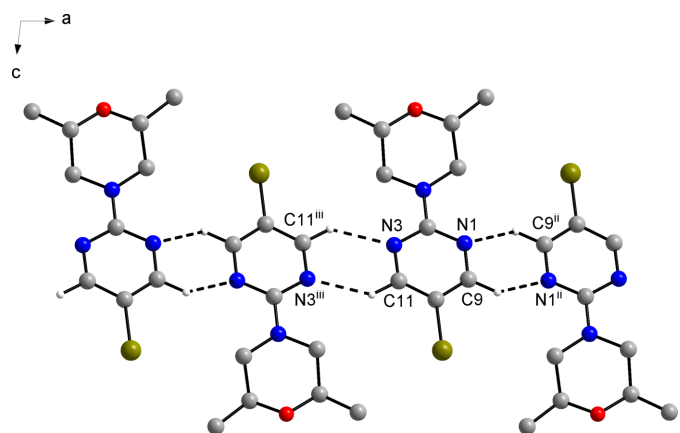


Figure 3
Part of the crystal structure of **4** viewed along the b -axis direction. H atoms not involved in C–H \cdots N weak hydrogen bonds are omitted for clarity. Dashed lines represent weak hydrogen bonds. Colour scheme: C, grey; H, white; Br, dark yellow; N, blue; O, red. Symmetry codes: (ii) $-x + 2, -y + 1, -z + 1$; (iii) $-x + 1, -y + 2, -z + 1$.

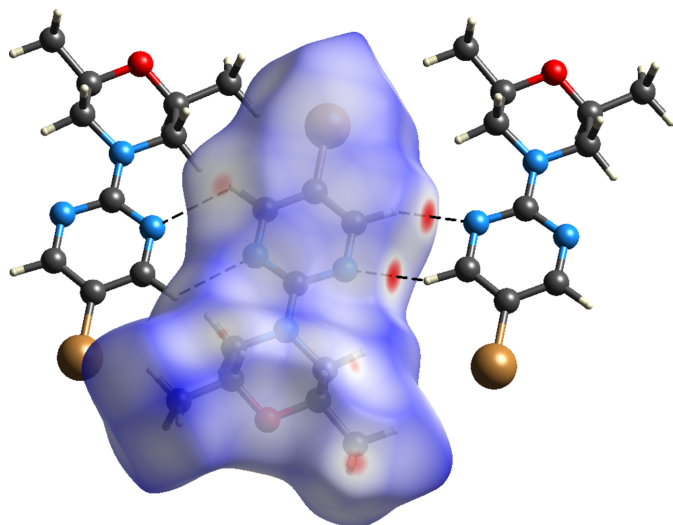


Figure 4
Hirshfeld surface mapped with d_{norm} for **4**. Colour scheme for the atoms: C, dark grey; H, white; Br, bronze; N, blue; O, red.

Waals radii (Bondi, 1964). Here, the two major red concave areas result from the $\text{C11} - \text{H11} \cdots \text{N3}^{\text{iii}}$ weak hydrogen bonds. Smaller red areas arise from the $\text{C9} - \text{H9} \cdots \text{N1}^{\text{ii}}$ and $\text{C7} - \text{H7A} \cdots \text{O1}^{\text{i}}$ short contacts as well as $\text{H} \cdots \text{H}$ intermolecular contacts involving the axial H atoms bonded to C2 and C6.

The corresponding two-dimensional fingerprint plot (Fig. 5) shows spikes from $\text{N} \cdots \text{H}/\text{H} \cdots \text{N}$ (11.5% of the surface area included), $\text{O} \cdots \text{H}/\text{H} \cdots \text{O}$ (5.2%) and $\text{Br} \cdots \text{H}/\text{H} \cdots \text{Br}$ contacts (19.1%) as well as wings from $\text{C} \cdots \text{H}/\text{H} \cdots \text{C}$ contacts (4.2%).

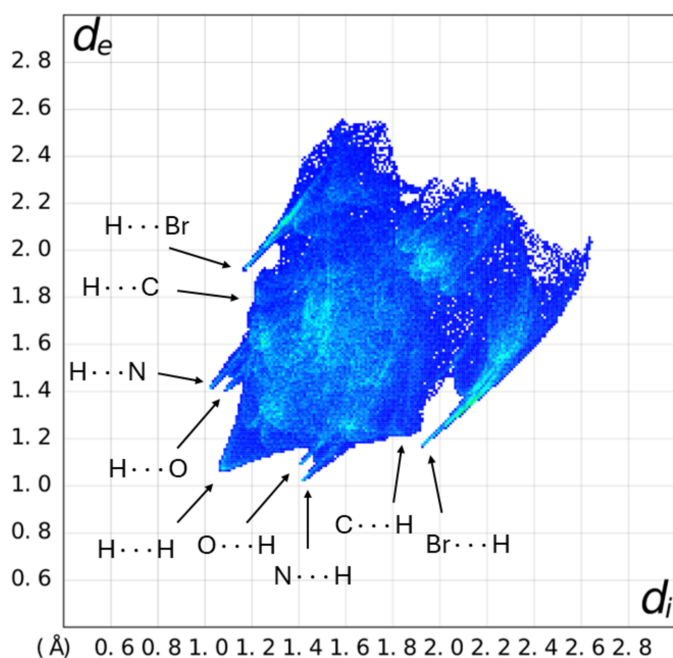


Figure 5
The two-dimensional fingerprint plot for **4**. d_i and d_e are the distances from the Hirshfeld surface to the nearest atoms inside and outside the surface, respectively. Dashed lines represent weak hydrogen bonds.

A triangular feature on the diagonal characteristic of face-to-face aromatic stacking is not observed, and $\text{C} \cdots \text{N}/\text{N} \cdots \text{C}$ and $\text{C} \cdots \text{C}$ contacts together only contribute 4.3% to the surface area included. $\text{H} \cdots \text{H}$ contacts account for 52.2% of the surface area. The tip on the diagonal centred at $d_c + d_i < 2.4 \text{ \AA}$ (*i.e.* less than twice the van der Waals radius of hydrogen) mirrors the small and weak red spots at the morpholine H atoms in the axial 2,6-positions in the d_{norm} plot in Fig. 4. A slight asymmetry about the diagonal in the fingerprint plot is noticeable, in particular for the $\text{Br} \cdots \text{H}/\text{H} \cdots \text{Br}$ spikes, which usually signals packing inefficiencies. Nonetheless, the packing index of 71% falls within the typical range observed for organic molecular crystals (Kitajgorodskij, 1973).

4. Database survey

The crystal structure most closely related to that of **4** in the Cambridge Structural Database (CSD; Groom *et al.*, 2016) is the structure of 4-(5-bromopyrimidin-2-yl)morpholine (ROTXOP; Cheprakova *et al.*, 2014). The corresponding 5-nitropyrimidine derivative has also been crystallographically characterized (YILPEQ; Gorbunov *et al.*, 2013). Therein, the coordination at the morpholine N atom is virtually planar [$\Sigma(\text{C}-\text{N}-\text{C}) = 360.0 (2)^\circ$], which can be attributed to the electron-withdrawing effect of the nitro group. As of June 2026, there are no examples of crystal structures containing 2,6-dimethylmorpholine with N-bound unsubstituted aromatic groups in the CSD, but a relatively large number of crystal structures containing an unsubstituted 4-phenylmorpholine moiety. In most of these crystal structures, the coordination at the morpholine N atom is markedly pyramidal, as in 4-phenylmorpholine (WOXMOP; Jiang *et al.*, 2023).

5. Synthesis and crystallization

General: Starting materials were purchased and used as received. 2,6-Dimethylmorpholine hydrochloride was obtained from BLDpharm. Solvents were distilled before use. NMR spectra were recorded on an Agilent Technologies 600 MHz shielded VNMRS and an Agilent Technologies 400 MHz VNMRS spectrometer. Chemical shifts are reported relative to the residual solvent signal of chloroform-*d* ($\delta_{\text{H}} = 7.26 \text{ ppm}$, $\delta_{\text{C}} = 77.16 \text{ ppm}$) or DMSO-*d*₆ ($\delta_{\text{H}} = 2.50 \text{ ppm}$, $\delta_{\text{C}} = 39.51 \text{ ppm}$). Abbreviations: *s* = singlet, *d* = doublet, *t* = triplet, *dd* = doublet of doublets, *dqd* = doublet of quartet of doublets, *m* = multiplet. HRMS data were acquired on a Thermo Scientific Q Exactive GC Orbitrap GC-MS system.

2,6-Dimethyl-4-(pyrimidin-2-yl)morpholine (3): 2-Chloropyrimidine (**1**) (5.73 g, 50.0 mmol) and 2,6-dimethylmorpholine hydrochloride (**2**) (7.59 g, 50.0 mmol) were suspended in 50 mL of ethanol and 15 mL of DIPEA were added with stirring. The mixture was heated to reflux for 7 h. Subsequently, the solvent was removed under reduced pressure and the residue was taken up with ethyl acetate (50 mL). After washing successively with water (30 mL) and brine (30 mL), the organic layer was dried over magnesium sulfate and the solvent was evaporated under reduced pressure. The

crude product was purified by flash chromatography (Interchim puriFlash[®] 430) on silica gel using gradient elution with *n*-heptane/ethyl acetate to yield **3** as a colourless oil (8.41 g, 44.0 mmol, 88%). ¹H NMR (600 MHz, chloroform-*d*) δ 8.31 (*d*, *J* = 4.8 Hz, 2H, H-4'/H-6'), 6.50 (*t*, *J* = 4.8 Hz, 1H, H-5'), 4.58–4.52 (*m*, 2H, H-3_{eq}/H-5_{eq}), 3.63 (*dqd*, *J* = 10.6, 6.3, 2.4 Hz, 2H, H-2_{ax}/H-6_{ax}), 2.60 (*dd*, *J* = 13.2, 10.6 Hz, 2H, H-3_{ax}/H-5_{ax}), 1.24 (*d*, *J* = 6.3 Hz, 6H, CH₃) ppm. ¹³C{¹H} NMR (151 MHz, chloroform-*d*): δ 161.1 (C-2'), 157.8 (C-4'/C-6'), 110.1 (C-5'), 71.9 (C-2/C-6), 49.5 (C-3/C-5), 19.0 (CH₃) ppm.

(2*R*,6*S*)-4-(5-Bromopyrimidin-2-yl)-2,6-dimethylmorpholine (**4**): Compound **3** (5.00 g, 26.1 mmol) was dissolved in 50 mL of dichloromethane and 0.80 mL (31.2 mmol) of bromine were added dropwise with stirring. After stirring for 12 h at room temperature, the progress of the reaction was checked by TLC. An additional 0.20 mL (7.8 mmol) of bromine was added and stirring was continued for 1 h. Subsequently, approx. 30 mL of a saturated aqueous sodium thiosulfate solution were added, whereupon the mixture became colourless. The organic layer was separated and the aqueous phase was extracted with dichloromethane (2 × 30 mL) followed by ethyl acetate (1 × 30 mL). After drying over magnesium sulfate, the combined organic layers were evaporated to dryness to obtain compound **4** as a white solid (6.58 g, 24.2 mmol, 93%). ¹H NMR (402 MHz, DMSO-*d*₆) δ 8.45 (*s*, 2H, H-4'/H-6'), 4.45–4.33 (*m*, 2H, H-3_{eq}/H-5_{eq}), 3.53 (*dqd*, *J* = 10.7, 6.2, 2.5 Hz, 2H, H-2_{ax}/H-6_{ax}), 2.52 (*dd*, *J* = 13.2, 10.7 Hz, 2H, H-3_{ax}/H-5_{ax}), 1.13 (*d*, *J* = 6.2 Hz, 6H, CH₃) ppm. ¹³C{¹H} APT NMR (101 MHz, DMSO-*d*₆): δ 159.2 (C-2'), 157.9 (C-4'/C-6'), 105.5 (C-5'), 70.8 (C-2/C-6), 48.9 (C-3/C-5), 18.6 (CH₃) ppm. HRMS(EI): *m/z* calculated for C₁₀H₁₄N₃OBr⁺ 271.031486 [*M*]⁺, found 271.031420. Crystals suitable for single-crystal X-ray diffraction analysis were grown from a solution in dichloromethane by slow evaporation of the solvent at ambient conditions.

6. Refinement details

Crystal data, data collection and structure refinement details are summarized in Table 2. The crystal structure was initially refined with *SHELXL* (Sheldrick, 2015*b*). Subsequently, Hirshfeld atom refinement was performed with *NoSpherA2* (Kleemiss *et al.*, 2021) in *OLEX2* (Dolomanov *et al.*, 2009). *ORCA* 6.1 (Neese, 2025) was used to calculate the electron density at the B3LYP/def2-TZVPP level of theory (Becke, 1993; Lee *et al.*, 1988; Weigend & Ahlrichs, 2005), which was partitioned into Hirshfeld atoms and converted *via* Fourier transform into atomic form factors (Midgley *et al.*, 2021). Least-squares refinements against the non-spherical atomic form factors thus obtained were carried out with *olex2.refine* (Bourhis *et al.*, 2015). Anisotropic atomic displacement parameters (ADPs) were introduced for all non-H atoms. Positions and isotropic ADPs of H atoms were refined freely.

The deviation from molecular point-group symmetry was calculated with *MOLSYM* in *PLATON* (Spek, 2009) using the atomic weighting mode. Hirshfeld surface analysis was conducted with *CrystalExplorer 21* (Spackman *et al.*, 2021),

Table 2

Experimental details.

Crystal data	
Chemical formula	C ₁₀ H ₁₄ BrN ₃ O
<i>M_r</i>	272.15
Crystal system, space group	Monoclinic, <i>P</i> 2 ₁ / <i>c</i>
Temperature (K)	100
<i>a</i> , <i>b</i> , <i>c</i> (Å)	10.3934 (6), 4.2323 (2), 25.8356 (14)
β (°)	97.076 (3)
<i>V</i> (Å ³)	1127.8 (1)
<i>Z</i>	4
Radiation type	Mo <i>K</i> α
μ (mm ⁻¹)	3.63
Crystal size (mm)	0.18 × 0.10 × 0.07
Data collection	
Diffractometer	Bruker AXS D8 VENTURE
Absorption correction	Gaussian (<i>SADABS</i> ; Krause <i>et al.</i> , 2015)
<i>T_{min}</i> , <i>T_{max}</i>	0.679, 0.860
No. of measured, independent and observed [<i>I</i> ≥ 2 σ (<i>I</i>)] reflections	97547, 3622, 3383
<i>R_{int}</i>	0.042
($\sin \theta/\lambda$) _{max} (Å ⁻¹)	0.727
Refinement	
$R[F^2 > 2\sigma(F^2)]$, $wR(F^2)$, <i>S</i>	0.013, 0.030, 1.06
No. of reflections	3622
No. of parameters	192
H-atom treatment	All H-atom parameters refined
$\Delta\rho_{\max}$, $\Delta\rho_{\min}$ (e Å ⁻³)	0.33, -0.24

Computer programs: *APEX6* (Bruker, 2024), *SAINT* (Bruker, 2019), *SHELXT* (Sheldrick, 2015*a*), *OLEX2.refine* (Bourhis *et al.*, 2015), *DIAMOND* (Brandenburg, 2018) and *publCIF* (Westrip, 2010).

which by default applies neutron-derived values for X–H bond lengths (Allen & Bruno, 2010).

Acknowledgements

We would like to thank Professor Christian W. Lehmann for providing access to the X-ray diffraction facility, Heike Salandin for technical assistance with the X-ray intensity data collection and Daniel Margold for measuring the HRMS data. We acknowledge the financial support of the Open Access Publication Fund of the Martin-Luther-Universität Halle-Wittenberg.

References

- Allen, F. H. & Bruno, I. J. (2010). *Acta Cryst.* **B66**, 380–386.
 Becke, A. D. (1993). *J. Chem. Phys.* **98**, 5648–5652.
 Bernstein, J., Davis, R. E., Shimon, L. & Chang, N. (1995). *Angew. Chem. Int. Ed. Engl.* **34**, 1555–1573.
 Bondi, A. (1964). *J. Phys. Chem.* **68**, 441–451.
 Bourhis, L. J., Dolomanov, O. V., Gildea, R. J., Howard, J. A. K. & Puschmann, H. (2015). *Acta Cryst.* **A71**, 59–75.
 Brandenburg, K. (2018). *DIAMOND*. Crystal Impact GbR, Bonn, Germany.
 Brügel, W. (1969). *Org. Magn. Reson.* **1**, 425–430.
 Bruker (2019). *SAINT*. Bruker AXS LLC, Madison, Wisconsin, USA.
 Bruker (2024). *APEX6*. Bruker AXS LLC, Madison, Wisconsin, USA.

- Cheprakova, E. M., Verbitskiy, E. V., Ezhikova, M. A., Kodess, M. I., Pervova, M. G., Slepukhin, P. A., Toporova, M. S., Kravchenko, M. A., Medvinskiy, I. D., Rusinov, G. L. & Charushin, V. N. (2014). *Russ. Chem. Bull.* **63**, 1350–1358.
- Desiraju, G. R. (1995). *Angew. Chem. Int. Ed. Engl.* **34**, 2311–2327.
- Dolomanov, O. V., Bourhis, L. J., Gildea, R. J., Howard, J. A. K. & Puschmann, H. (2009). *J. Appl. Cryst.* **42**, 339–341.
- Gorbunov, E. B., Novikova, R. K., Plekhanov, P. V., Slepukhin, P. A., Rusinov, G. L., Rusinov, V. L., Charushin, V. N. & Chupakhin, O. N. (2013). *Chem. Heterocycl. Cmpd* **49**, 766–775.
- Groom, C. R., Bruno, I. J., Lightfoot, M. P. & Ward, S. C. (2016). *Acta Cryst.* **B72**, 171–179.
- Hall, J. R., Romer, N. P., Spiller, T. E., Sigman, M. S. & Sanford, M. S. (2025). *Chem. Sci.* **16**, 18936–18941.
- Hanyu, N., Saito, T., Shibata, T., Sato, K. & Ogino, K. (2009). Shiseido Co Ltd. WO20090991912A1.
- Heng, R., Koch, G., Schlapbach, A. & Seiler, M. P. (2008). Novartis A.-G. WO2008034600A1.
- Jiang, D., Lu, T., Du, C., Liu, F., Yan, Z., Hu, D., Shang, A., Gao, L., Lu, P. & Ma, Y. (2023). *Sci. China Chem.* **66**, 1132–1138.
- Kitajgorodskij, A. I. (1973). *Molecular crystals and molecules*. New York: Academic Press.
- Kleemiss, F., Dolomanov, O. V., Bodensteiner, M., Peyerimhoff, N., Midgley, L., Bourhis, L. J., Genoni, A., Malaspina, L. A., Jayatilaka, D., Spencer, J. L., White, F., Grundkötter-Stock, B., Steinhauer, S., Lentz, D., Puschmann, H. & Grabowsky, S. (2021). *Chem. Sci.* **12**, 1675–1692.
- Krause, L., Herbst-Irmer, R., Sheldrick, G. M. & Stalke, D. (2015). *J. Appl. Cryst.* **48**, 3–10.
- Lee, C., Yang, W. & Parr, R. G. (1988). *Phys. Rev. B* **37**, 785–789.
- Midgley, L., Bourhis, L. J., Dolomanov, O. V., Grabowsky, S., Kleemiss, F., Puschmann, H. & Peyerimhoff, N. (2021). *Acta Cryst.* **A77**, 519–533.
- Neese, F. (2025). *WIREs Comput. Mol. Sci.* **15**, e70019.
- Palme, P. R., Grover, S., Abdelaziz, R., Mann, L., Kany, A. M., Ouologuem, L., Bartel, K., Sonnenkalb, L., Reiling, N., Hirsch, A. K. H., Schnappinger, D., Rubinstein, J. L., Imming, P. & Richter, A. (2025). *J. Med. Chem.* **68**, 25274–25289.
- Sheldrick, G. M. (2015a). *Acta Cryst.* **A71**, 3–8.
- Sheldrick, G. M. (2015b). *Acta Cryst.* **C71**, 3–8.
- Shojaei, F., Fang, C., Semple, J. E. & Gillings, M. (2023). Huyabio International LLC. WO2023177592A1.
- Spackman, M. A. & Jayatilaka, D. (2009). *CrystEngComm* **11**, 19–32.
- Spackman, P. R., Turner, M. J., McKinnon, J. J., Wolff, S. K., Grimwood, D. J., Jayatilaka, D. & Spackman, M. A. (2021). *J. Appl. Cryst.* **54**, 1006–1011.
- Spek, A. L. (2009). *Acta Cryst.* **D65**, 148–155.
- Wei, X., Zhang, C., Wang, Y., Zhan, Q., Qiu, G., Fan, L. & Yin, G. (2019). *Eur. J. Org. Chem.* **2019**, 7142–7150.
- Weigend, F. & Ahlrichs, R. (2005). *Phys. Chem. Chem. Phys.* **7**, 3297–3305.
- Westrip, S. P. (2010). *J. Appl. Cryst.* **43**, 920–925.
- Wu, H., Lin, J., Li, Y., Wei, C. & Chen, S. (2015). Medshine Discovery Inc. CN104945377 A.
- Yoshihara, K., Suzuki, D., Yamaki, S., Koga, Y., Seki, N., Fujiyasu, J. & Neya, M. (2011). Astellas Pharma Inc. WO2011034078A1.
- You, Q., Guo, X., Shojaei, F., Chen, X., Semple, J. E., Jiang, Z., Xu, X. & Gillings, M. (2023). Huyabio International LLC, China Pharmaceutical University. US20230286925A1.
- Yuan, C., Jia, C., Zhang, X., Zhang, W., You, Y., Xu, X., Zhu, L., Chen, Y., Dong, Y. & Xu, L. (2024). *Org. Lett.* **26**, 4877–4881.

supporting information

Acta Cryst. (2026). E82, 768-772 [https://doi.org/10.1107/S2056989026006158]

Crystal structure of the *meso* compound (2*R*,6*S*)-4-(5-bromopyrimidin-2-yl)-2,6-dimethylmorpholine

Paul R. Palme, Richard Goddard, Markus Leutzsch, Adrian Richter, Peter Imming and Rüdiger W. Seidel

Computing details

(2*R*,6*S*)-4-(5-Bromopyrimidin-2-yl)-2,6-dimethylmorpholine

Crystal data

$C_{10}H_{14}BrN_3O$

$M_r = 272.15$

Monoclinic, $P2_1/c$

$a = 10.3934$ (6) Å

$b = 4.2323$ (2) Å

$c = 25.8356$ (14) Å

$\beta = 97.076$ (3)°

$V = 1127.8$ (1) Å³

$Z = 4$

$F(000) = 551.505$

$D_x = 1.603$ Mg m⁻³

Mo $K\alpha$ radiation, $\lambda = 0.71073$ Å

Cell parameters from 9300 reflections

$\theta = 3.2$ – 31.0 °

$\mu = 3.63$ mm⁻¹

$T = 100$ K

Prism, colourless

$0.18 \times 0.10 \times 0.07$ mm

Data collection

Bruker AXS D8 VENTURE

diffractometer

Radiation source: $I\mu S$ Diamond

Incoatec Helios mirrors monochromator

Detector resolution: 7.391 pixels mm⁻¹

φ and ω scans

Absorption correction: gaussian
(SADABS; Krause *et al.*, 2015)

$T_{\min} = 0.679$, $T_{\max} = 0.860$

97547 measured reflections

3622 independent reflections

3383 reflections with $I \geq 2\sigma(I)$

$R_{\text{int}} = 0.042$

$\theta_{\max} = 31.1$ °, $\theta_{\min} = 2.0$ °

$h = -15 \rightarrow 15$

$k = -6 \rightarrow 6$

$l = -37 \rightarrow 37$

Refinement

Refinement on F^2

Least-squares matrix: full

$R[F^2 > 2\sigma(F^2)] = 0.013$

$wR(F^2) = 0.030$

$S = 1.06$

3622 reflections

192 parameters

0 restraints

0 constraints

Primary atom site location: dual

Secondary atom site location: difference Fourier map

Hydrogen site location: difference Fourier map

All H-atom parameters refined

$w = 1/[\sigma^2(F_o^2) + (0.0129P)^2 + 0.1241P]$

where $P = (F_o^2 + 2F_c^2)/3$

$(\Delta/\sigma)_{\max} = -0.0001$

$\Delta\rho_{\max} = 0.33$ e Å⁻³

$\Delta\rho_{\min} = -0.24$ e Å⁻³

Special details

Experimental. Crystal mounted on a MiTeGen loop using Perfluoropolyether PFO-XR75

Refinement. Refinement using NoSpherA2, an implementation of Non-SPHERical Atom-form-factors in Olex2. Please cite: F. Kleemiss *et al.* Chem. Sci. DOI 10.1039/D0SC05526C - 2021 NoSpherA2 implementation of HAR makes use of tailor-made aspherical atomic form factors calculated on-the-fly from a Hirshfeld-partitioned electron density (ED) - not from spherical-atom form factors.

The ED is calculated from a gaussian basis set single determinant SCF wavefunction - either Hartree-Fock or DFT using selected functionals - for a fragment of the crystal. This fragment can be embedded in an electrostatic crystal field by employing cluster charges or modelled using implicit solvation models, depending on the software used.

The following options were used: SOFTWARE: ORCA 6.1 PARTITIONING: NoSpherA2 INT ACCURACY: Normal METHOD: B3LYP BASIS SET: def2-TZVPP CHARGE: 0 MULTIPLICITY: 1 DATE: 2026-04-01_20-42-29

The minimum and maximum estimated transmissions from the multi-scan scaling are 0.6613 and 0.8743 (SADABS).

Fractional atomic coordinates and isotropic or equivalent isotropic displacement parameters (\AA^2)

	<i>x</i>	<i>y</i>	<i>z</i>	$U_{\text{iso}}^*/U_{\text{eq}}$
C1	0.86770 (7)	0.35247 (18)	0.28616 (3)	0.02637 (14)
H1A	0.8346 (11)	0.407 (2)	0.2447 (5)	0.049 (3)*
H1B	0.8798 (11)	0.100 (2)	0.2894 (4)	0.048 (3)*
H1C	0.9610 (11)	0.460 (3)	0.2975 (4)	0.051 (3)*
C2	0.76932 (6)	0.47733 (16)	0.31971 (3)	0.02041 (12)
H2	0.7597 (9)	0.736 (2)	0.3144 (4)	0.034 (2)*
C3	0.80623 (6)	0.40775 (17)	0.37755 (3)	0.02130 (12)
H3A	0.8193 (10)	0.150 (2)	0.3831 (4)	0.040 (3)*
H3B	0.8993 (9)	0.525 (2)	0.3919 (4)	0.034 (2)*
C5	0.57364 (6)	0.42407 (17)	0.38639 (3)	0.02103 (12)
H5A	0.5027 (10)	0.546 (2)	0.4076 (4)	0.039 (2)*
H5B	0.5608 (10)	0.170 (2)	0.3940 (4)	0.039 (3)*
C6	0.54734 (6)	0.48648 (16)	0.32811 (3)	0.01974 (12)
H6	0.5531 (8)	0.746 (2)	0.3220 (3)	0.032 (2)*
C7	0.41680 (7)	0.36042 (17)	0.30472 (3)	0.02331 (13)
H7A	0.3993 (11)	0.410 (3)	0.2635 (5)	0.056 (3)*
H7B	0.3402 (11)	0.467 (3)	0.3244 (5)	0.053 (3)*
H7C	0.4119 (11)	0.106 (2)	0.3097 (4)	0.048 (3)*
C8	0.73225 (6)	0.65197 (15)	0.45507 (2)	0.01870 (11)
C9	0.88456 (6)	0.79021 (17)	0.52262 (3)	0.02176 (12)
H9	0.9834 (10)	0.791 (3)	0.5395 (4)	0.043 (2)*
C10	0.78849 (6)	0.91794 (15)	0.54884 (2)	0.01989 (12)
C11	0.66181 (6)	0.90051 (17)	0.52476 (3)	0.02281 (13)
H11	0.5802 (10)	0.999 (3)	0.5425 (4)	0.047 (3)*
Br1	0.829245 (7)	1.105440 (18)	0.615057 (3)	0.02623 (3)
N1	0.85771 (5)	0.65779 (14)	0.47578 (2)	0.02223 (11)
N3	0.63261 (5)	0.76677 (15)	0.47811 (2)	0.02287 (11)
N4	0.70440 (5)	0.52684 (15)	0.40639 (2)	0.02233 (11)
O1	0.64614 (4)	0.34162 (11)	0.302198 (18)	0.02004 (9)

Atomic displacement parameters (Å²)

	U^{11}	U^{22}	U^{33}	U^{12}	U^{13}	U^{23}
C1	0.0264 (3)	0.0294 (4)	0.0253 (3)	-0.0036 (3)	0.0111 (3)	-0.0039 (3)
C2	0.0226 (3)	0.0190 (3)	0.0205 (3)	-0.0011 (2)	0.0062 (2)	-0.0007 (2)
C3	0.0178 (3)	0.0270 (3)	0.0197 (3)	0.0014 (2)	0.0045 (2)	-0.0018 (2)
C5	0.0168 (3)	0.0271 (3)	0.0194 (3)	0.0011 (2)	0.0027 (2)	0.0002 (2)
C6	0.0206 (3)	0.0179 (3)	0.0203 (3)	0.0019 (2)	0.0011 (2)	0.0004 (2)
C7	0.0212 (3)	0.0234 (3)	0.0244 (3)	0.0028 (2)	-0.0009 (2)	-0.0021 (2)
C8	0.0149 (3)	0.0239 (3)	0.0175 (3)	0.0030 (2)	0.0029 (2)	0.0010 (2)
C9	0.0153 (3)	0.0303 (3)	0.0196 (3)	0.0036 (2)	0.0019 (2)	-0.0023 (2)
C10	0.0182 (3)	0.0245 (3)	0.0173 (3)	0.0035 (2)	0.0033 (2)	-0.0004 (2)
C11	0.0169 (3)	0.0325 (3)	0.0193 (3)	0.0064 (2)	0.0036 (2)	-0.0016 (3)
Br1	0.02647 (4)	0.03261 (4)	0.01976 (4)	0.00209 (3)	0.00346 (2)	-0.00558 (3)
N1	0.0148 (2)	0.0317 (3)	0.0204 (3)	0.0039 (2)	0.00277 (19)	-0.0036 (2)
N3	0.0151 (2)	0.0347 (3)	0.0190 (2)	0.0052 (2)	0.00271 (19)	-0.0018 (2)
N4	0.0155 (2)	0.0329 (3)	0.0189 (3)	0.0012 (2)	0.00342 (19)	-0.0032 (2)
O1	0.0220 (2)	0.0190 (2)	0.0194 (2)	0.00032 (17)	0.00371 (17)	-0.00088 (17)

Geometric parameters (Å, °)

C1—H1A	1.108 (11)	C6—C7	1.5128 (9)
C1—H1B	1.079 (10)	C6—O1	1.4310 (8)
C1—H1C	1.078 (11)	C7—H7A	1.078 (12)
C1—C2	1.5147 (9)	C7—H7B	1.094 (11)
C2—H2	1.105 (10)	C7—H7C	1.085 (10)
C2—C3	1.5250 (10)	C8—N1	1.3473 (8)
C2—O1	1.4252 (8)	C8—N3	1.3471 (8)
C3—H3A	1.107 (10)	C8—N4	1.3626 (8)
C3—H3B	1.109 (10)	C9—H9	1.065 (10)
C3—N4	1.4572 (8)	C9—C10	1.3838 (9)
C5—H5A	1.101 (10)	C9—N1	1.3315 (9)
C5—H5B	1.104 (10)	C10—C11	1.3872 (9)
C5—C6	1.5201 (9)	C10—Br1	1.8860 (7)
C5—N4	1.4595 (8)	C11—H11	1.095 (11)
C6—H6	1.111 (10)	C11—N3	1.3321 (9)
H1B—C1—H1A	107.5 (8)	O1—C6—C5	109.70 (5)
H1C—C1—H1A	109.7 (8)	O1—C6—H6	107.6 (4)
H1C—C1—H1B	107.6 (8)	O1—C6—C7	108.79 (5)
C2—C1—H1A	109.2 (6)	H7A—C7—C6	111.1 (6)
C2—C1—H1B	112.4 (6)	H7B—C7—C6	109.7 (6)
C2—C1—H1C	110.3 (6)	H7B—C7—H7A	109.6 (9)
H2—C2—C1	109.3 (5)	H7C—C7—C6	110.8 (6)
C3—C2—C1	112.79 (6)	H7C—C7—H7A	107.7 (8)
C3—C2—H2	108.7 (5)	H7C—C7—H7B	107.8 (8)
O1—C2—C1	108.73 (5)	N3—C8—N1	125.24 (6)
O1—C2—H2	107.2 (5)	N4—C8—N1	117.32 (5)

O1—C2—C3	109.93 (5)	N4—C8—N3	117.42 (6)
H3A—C3—C2	109.2 (6)	C10—C9—H9	121.0 (5)
H3B—C3—C2	110.2 (5)	N1—C9—H9	117.2 (5)
H3B—C3—H3A	108.0 (7)	N1—C9—C10	121.75 (6)
N4—C3—C2	108.86 (5)	C11—C10—C9	117.51 (6)
N4—C3—H3A	111.1 (5)	Br1—C10—C9	120.90 (5)
N4—C3—H3B	109.5 (5)	Br1—C10—C11	121.60 (5)
H5B—C5—H5A	105.4 (7)	H11—C11—C10	122.2 (6)
C6—C5—H5A	111.2 (5)	N3—C11—C10	121.75 (6)
C6—C5—H5B	109.6 (5)	N3—C11—H11	116.0 (6)
N4—C5—H5A	109.6 (5)	C9—N1—C8	116.93 (6)
N4—C5—H5B	110.8 (5)	C11—N3—C8	116.82 (6)
N4—C5—C6	110.17 (5)	C5—N4—C3	114.79 (5)
H6—C6—C5	107.9 (4)	C8—N4—C3	121.42 (5)
C7—C6—C5	112.17 (6)	C8—N4—C5	121.68 (5)
C7—C6—H6	110.6 (4)	C6—O1—C2	110.32 (5)
C1—C2—C3—N4	-178.16 (6)	C7—C6—C5—N4	175.48 (6)
C1—C2—O1—C6	-172.02 (5)	C8—N1—C9—C10	-0.37 (7)
C2—C3—N4—C5	51.43 (6)	C8—N3—C11—C10	-0.71 (7)
C2—C3—N4—C8	-144.83 (5)	C9—C10—C11—N3	-0.09 (8)
C2—O1—C6—C5	-62.59 (5)	C9—N1—C8—N3	-0.53 (8)
C2—O1—C6—C7	174.37 (5)	C9—N1—C8—N4	177.77 (6)
C3—C2—O1—C6	64.06 (6)	C11—C10—C9—N1	0.66 (8)
C3—N4—C5—C6	-50.89 (6)	C11—N3—C8—N1	1.07 (8)
C3—N4—C8—N1	-0.77 (7)	C11—N3—C8—N4	-177.23 (6)
C3—N4—C8—N3	177.67 (6)	Br1—C10—C9—N1	-179.78 (5)
C5—N4—C8—N1	161.85 (6)	Br1—C10—C11—N3	-179.64 (5)
C5—N4—C8—N3	-19.71 (7)	N4—C3—C2—O1	-56.64 (6)
C6—C5—N4—C8	145.42 (5)	N4—C5—C6—O1	54.47 (6)

Hydrogen-bond geometry (\AA , $^\circ$)

$D-H\cdots A$	$D-H$	$H\cdots A$	$D\cdots A$	$D-H\cdots A$
C7—H7A \cdots O1 ⁱ	1.078 (12)	2.499 (12)	3.4295 (9)	143.9 (8)
C9—H9 \cdots N1 ⁱⁱ	1.065 (10)	2.580 (10)	3.2779 (9)	122.5 (7)
C11—H11 \cdots N3 ⁱⁱⁱ	1.095 (11)	2.423 (11)	3.3610 (9)	142.8 (8)

Symmetry codes: (i) $-x+1, y+1/2, -z+1/2$; (ii) $-x+2, -y+1, -z+1$; (iii) $-x+1, -y+2, -z+1$.